Oxygen impurities in X-ray storage phosphors BaFBr and BaFCl investigated by ^{17}O NMR

1994 J. Phys.: Condens. Matter 6 8633

(http://iopscience.iop.org/0953-8984/6/41/025)

J. Phys.: Condens. Matter 6 (1994) 8633–8644. Printed in the UK

Oxygen impurities in x-ray storage phosphors BaFBr and BaFCl investigated by ^{17}O NMR

T J Bastow†, S N Stuart†, W G McDugle‡, R S Eachus‡ and J M Spaeth§

† Division of Materials Science and Technology, CSIRO Australia, Clayton, Victoria 3169, Australia

‡ Research Laboratories, Eastman Kodak Company, Rochester, New York 14650-2021, USA

§ Fachbereich Physik, University of Paderborn, 33095 Paderborn, Germany

Received 2 August 1994

Abstract. Magic-angle-spinning nuclear magnetic resonance (NMR) spectroscopy of BaFBr and BaFCl doped with up to 6 mol.% oxygen (previously enriched to 40% in ^{17}O) has detected sites on which oxygen impurities were incorporated. In BaFBr:O, monatomic O^{2-} is found preferentially on fluoride sites, and subsidiarily on bromide sites, but in BaFCl:O, substitutional O^{2-} falls below the threshold of detection. In both systems the diamagnetic molecular anion O_2^{2-} is detected, on one site in BaFBr:O, on two in BaFCl:O; one of the latter is assigned to the chloride site, while the other is attributed to interstitial O_2^{2-}. Although it was intended to introduce oxygen only through BaO, ^{1}H NMR indicates OH^- on several sites. The NMR spectra, including those of ^{19}F, ^{81}Br and ^{35}Cl, are compared with results obtained previously by electron paramagnetic resonance and magneto-optical techniques on ^{17}O-containing, x-irradiated samples.

1. Introduction

X-ray storage phosphors are materials capable of recording an image created by the absorption of x-radiation. The best known examples are barium fluorobromide, BaFBr, and barium fluorochloride, BaFCl, doped with divalent europium ions (Stevels and Pingault 1975, Luckey 1975, 1983, Kotera *et al* 1980, Sonoda *et al* 1983, Amemiya and Miyahara 1988). The precise mechanism of image production is not yet fully understood. It is accepted that room-temperature-stable trapped electron and hole centres generated by the x-irradiation are involved in the imaging process. In these BaFX materials, where X denotes Cl or Br, the electron centres are trapped at either X^- or F^- vacancies, producing F(X^-) or F(F^-) centres. Upon optical excitation in the F-centre absorption band during the read-out process, the electrons recombine with the trapped hole centres, which results in the characteristic Eu^{2+} emission at 390 nm (i.e., photo-stimulated luminescence or PSL). The identity of the stable hole centre involved in imaging and the exact nature of the read-out mechanism are still controversial and not yet understood (Takahashi *et al* 1984, 1985, Seggern *et al* 1988a, b, Hangleiter *et al* 1990).

It has recently been demonstrated by electron paramagnetic resonance (EPR) spectroscopy that BaFX materials include oxygen as an ubiquitous impurity (Koschnick *et al* 1991, Eachus *et al* 1991a). EPR demonstrated the presence of O^{2-} ions in both materials. During preparation of polycrystalline powders or single crystals, BaFBr and BaFCl scavenge oxygen from their growth environment so that pure samples are difficult to produce (Eachus *et al* 1993a, 1993b).

0953-8984/94/418633+12$19.50

The BaFX materials share the tetragonal matlockite structure of PbFCl (Sauvage 1974, Liebich and Nicollin 1977, Beck 1979) which is shown in figure 1. The monatomic divalent anion O^{2-} may be incorporated on either the F^- or X^- sites, accompanied by an X^- or F^- vacancy, respectively, for charge compensation. Upon x-irradiation, O^{2-} traps a hole by reacting with the mobile Br_2^- V_K centre, and forms the paramagnetic centres O_F^- and O_X^-, where the subscript denotes the site of substitution. By doping the crystal with oxygen enriched with the magnetic isotope ^{17}O (nuclear spin $I = 5/2$), it has been possible to measure and analyse EPR and electron nuclear double resonance (ENDOR) spectra of the oxygen centres (Eachus *et al* 1991a, b, Eachus *et al* to be published). Although only substitutional O^{2-} centres have been detected in BaFX, in principle, O^{2-} could also be incorporated at interstitial positions, with various vacancy sites available for charge compensation. By capturing the holes generated by x-irradiation, the oxide impurities affect imaging, even though they may not be directly involved in the recombination process giving rise to the PSL (Koschnick 1991, Eachus *et al* 1993a). Oxide incorporation also increases the yield of stable F(Br^-) centres involved in the PSL process.

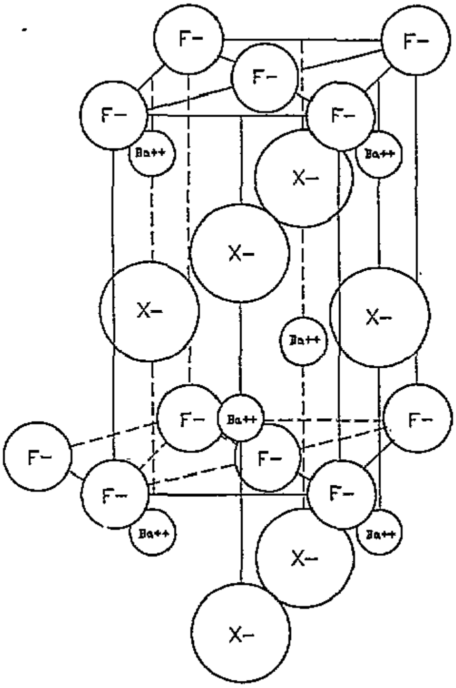

Figure 1. Matlockite structure of BaFX (X = Br, Cl) crystals.

Monatomic oxide is not the only oxygen-bearing impurity in the barium fluorohalides. Recently, it was shown by EPR that x-irradiation of as-grown BaFCl produces $(O_2^-)_{Cl}$ centres, superoxide radical anions on chloride sites (Eachus *et al* 1993b). Hole trapping by substitutional peroxide anions O_2^{2-} was assumed to be the generation mechanism for this centre. Interestingly, analogous $(O_2^-)_{Br}$ centres have not been detected in BaFBr.

The above observations using EPR techniques were restricted to the detection of paramagnetic species created by x-irradiation of as-grown materials. For a better understanding of x-ray imaging in these storage phosphors, it is important to investigate thoroughly the structure and location of oxygen-related, diamagnetic precursors to the trapped hole centres. The possibility of detecting oxygen-bearing impurities in their diamagnetic forms in unirradiated material is offered by nuclear magnetic resonance (NMR) spectroscopy. It is the purpose of this paper to report high-resolution NMR measurements of $^{17}O^{2-}$ doped into BaFX up to an oxygen content of 6 mol.%. It may be noted that ^{17}O NMR observations of oxygen species occurring at less than 10 atom-percent in inorganic materials is unusual. Our aim, guided by the EPR experience, is to identify the oxygen species that appear in the NMR.

2. Experimental procedure

2.1. Material preparation

Mixtures of optical-grade barium fluoride (Harshaw/Filtrol) and barium bromide or chloride (APL Engineered Materials, 5N purity) were first melted together under high vacuum and then treated with high purity bromine (or chlorine) in an ultra-pure carrier grade argon stream (Air Products) for several hours. For oxide doping, anhydrous barium oxide was prepared from finely dispersed barium metal and H_2O. The metal was obtained from the controlled thermal decomposition of barium azide in high vacuum and 41% $H_2\,^{17}O$ was used to achieve isotopic enrichment. The finely dispersed BaO was mixed with the halogen-purified BaFX (X = Br, Cl) in a boron nitride crucible, heated to 800 °C under high vacuum, melted under ultra-pure carrier grade argon, then quenched by removing the quartz tube containing the samples from the vertical furnace and plunging the sample zone into distilled water. Doping levels of 2, 3 and 6% were selected for BaFBr:O, and 6% for BaFCl:O; these figures signify the mole fraction of BaO in the mixture. BaFX:O powders of particle size 50–100 μm were prepared by this means.

One sample of BaFBr:O (3%) was annealed under dry nitrogen by heating for 12 h to 325 °C, then for 2 h to 880 °C, holding that temperature for 4 h and slowly cooling to room temperature. A sample of BaFBr:O (6%) at room temperature was exposed for 30 min on a rotating stage to white radiation from a copper x-ray tube operating at 1.35 kW.

Aged samples of BaFX:O and commercial grades of $BaX_2{\cdot}2H_2O$ were prepared for ^1H study by warming at 336 K for 40 h in air.

2.2. NMR spectroscopy

NMR spectra were recorded with a Bruker MSL 400 spectrometer working in a field of 9.4 T. Operating frequencies of 400.2, 374.3, 108.0, 54.26 and 39.19 MHz allowed observation of ^1H, ^{19}F, ^{81}Br, ^{17}O and ^{35}Cl spectra, respectively. External frequency standards were taken from $Si(CH_3)_4$, NaF, H_2O and NaCl. Magic-angle spinning (MAS) was done in a spinner, of capacity 0.3 ml (7 mm o.d.) for ^{17}O spectra, and 0.1 ml (4 mm o.d.) for ^1H and ^{19}F spectra, driven by a Bruker double bearing gas turbine; the rotation frequency was set between 3.5 and 47 kHz (^{17}O spectra) or between 7.5 and 12 kHz (^1H and ^{19}F spectra). The ^{17}O spectra were obtained from the free decay of magnetization following a single 1.6 μs RF pulse, employing phase-cycled quadrature detection, with repetition period 10 to 30 s. Nutation of ^{17}O magnetization in the RF field near resonance was investigated by varying the exciting pulse length up to 8 μs. The longitudinal relaxation time was estimated by progressive saturation, and the transverse relaxation time was measured by the two-pulse Carr–Purcell spin echo. Static spectra of ^1H were obtained with a single 1 μs pulse, and those of ^{81}Br

and ^{35}Cl with a solid echo pulse sequence. The NMR experiments were performed at room temperature, except for ^{17}O spectroscopy of BaFBr:O (3%) at 360 and 220 K.

BaFBr:O (3%) was also examined in a field of 11.7 T using an MSL 500: the ^{17}O spectrum was observed at 67.82 MHz with pulse length of 0.8 μs, repetition period 2 s, MAS frequency 5.0 kHz.

3. Results

3.1. *Halogen NMR*

The ^{19}F MAS spectrum of each system showed a single resonance: the chemical shift was 209.1 ppm for BaFBr:O (2%), 213.2 ppm for BaFCl:O (6%); and the linewidth (FWHM) was 0.7 and 0.8 kHz, respectively. Both were sharper than the ^{19}F MAS line in barium fluoride at 210.6 ppm, width 1.4 kHz, and in sodium fluoride, width 1.9 kHz. Figure 2 shows spectra of the other halogen species in the crystals: they are static powder patterns of the central transition of (a) ^{81}Br and (b) ^{35}Cl and have well defined lineshape with a peak separation of 120.5 and 18.8 kHz, respectively. The lineshape is due to second-order quadrupole interaction (Cohen and Reif 1957) and corresponds to a coupling constant of 10.00 MHz for ^{81}Br and 2.38 MHz for ^{35}Cl. The asymmetry parameter is zero, by site symmetry. Evidently the introduction of oxygen has not appreciably degraded the crystalline order.

3.2. *^{17}O NMR of BaFBr:O*

Figure 3 shows the ^{17}O NMR spectrum of BaFBr:O. There are two groups of lines, four sharp (consisting of two pairs of different intensity) about 600 ppm and one broader about 200 ppm, as well as the line at 378 ppm from the partially stabilized zirconia of the spinner tube (mass, 1.6 g) (Bastow and Stuart 1990) with its series of spinning sidebands (marked by asterisks in the figure). Table 1 presents the chemical shifts (δ' not corrected for quadrupole interaction) and linewidths, in terms of relative frequency, and relative integrated centre band intensities from the absorption spectrum (figure 3, with intensities corrected for finite repetition time and sideband interference). The spectra of oxygen content 2, 3 and 6% differed only in the pattern of intensities, which is shown graphically in figure 4. The main effects are the decay of the line at 587 ppm and the growth of the line at 610 ppm as oxygen is added. In the spectrum recorded at higher field (not shown), line positions were the same and the line at 198 ppm was no narrower. When the pulse length was increased from 1.6 to 4 μs, the lines at 610 and 587 ppm were definitely reduced. Rough measurement of the spin–lattice relaxation time shows values of several seconds (table 1). The linewidth imposes an upper bound on the strength of the quadrupole interaction, as measured by the parameter $hK_Q = e^2|qQ|(1+\frac{1}{3}\eta^2)^{1/2}$ (Bastow and Stuart 190), which is included in table 1.

The x-irradiation produced no effect on the spectrum collected over one hour promptly following the exposure.

Temperature variation showed no significant shift in position of the three strongest lines. After annealing (see section 2.1), the four lines at about 600 ppm completely disappeared and the broader line increased marginally in intensity.

In samples stored at room temperature, the broader line was found to decay with a time constant estimated as 190 d (oxygen content 3%) or 120 d (oxygen content 6%), while the other intensities changed much more slowly.

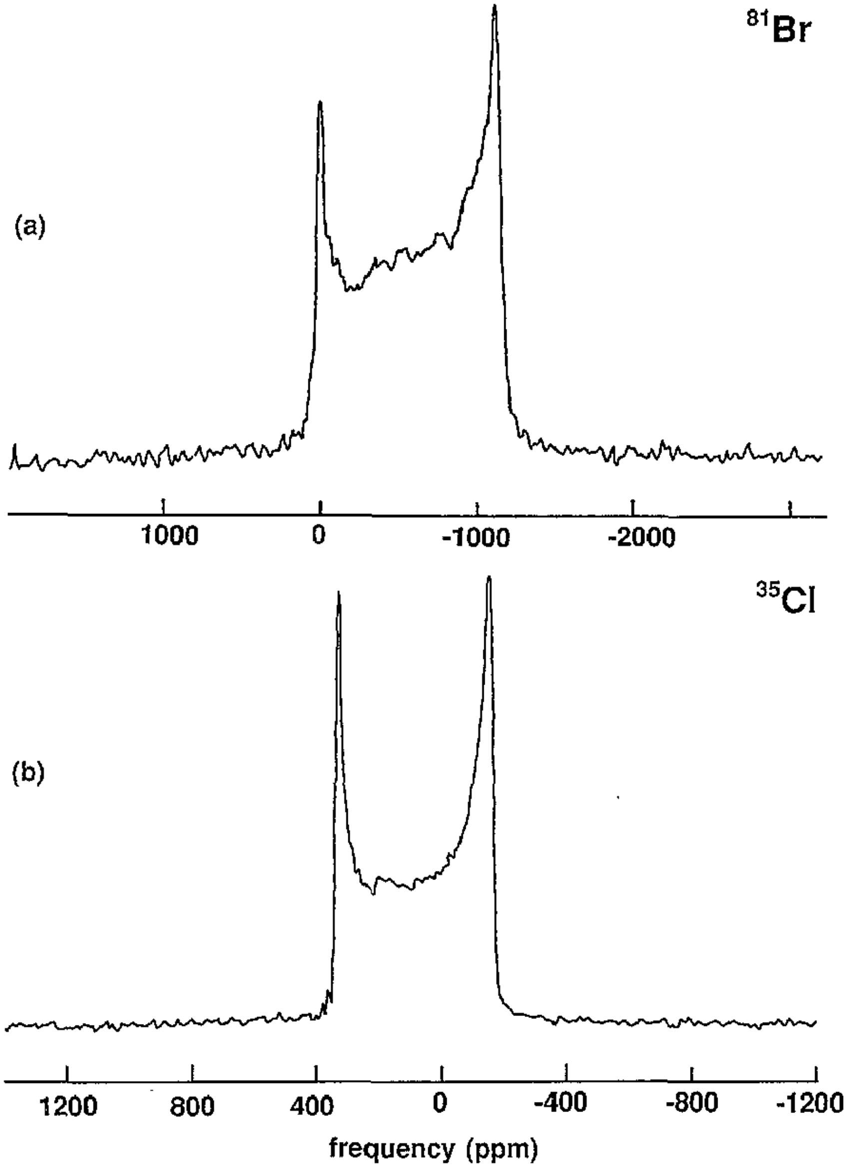

Figure 2. NMR spectra of (a) ^{81}Br in BaFBr:O (2%), (b) ^{35}Cl in BaFCl:O (6%), static powder patterns. Field is 9.4 T; frequency reference for ^{81}Br is arbitrary.

3.3. ^{17}O NMR of BaFCl:O

Figure 5 shows the ^{17}O MAS spectrum of BaFCl:O. This spectrum, which is obtained with very good signal-to-noise ratio, shows lines only in the region of 170 ppm and some absorption about 0 ppm, in contrast to the case of BaFBr:O. There is an extensive series of spinning sidebands of low intensity. The spectral parameters are given in table 1. The nutation experiment, with RF rotating amplitude $\nu_1 = 58$ kHz, showed all three lines attaining their maximum about 2.4 times earlier than in water. In addition, spin echo spectra, with curve fitting to separate the overlapping lines at 181 and 161 ppm, yielded $T_2 = 20$, 12 ms,

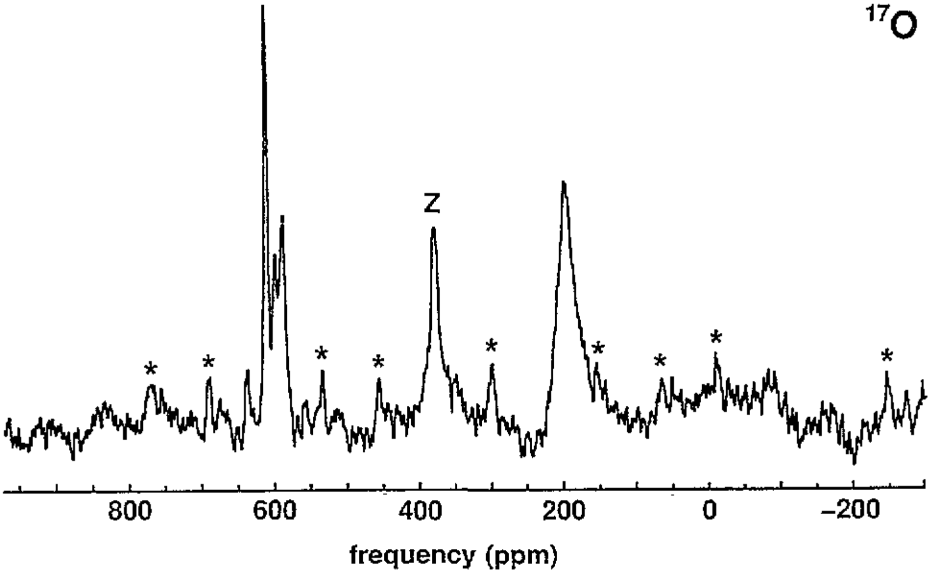

Figure 3. NMR spectrum of ^{17}O in BaFBr:O (3%) unde magic-angle spinning in zirconia spinner (Z), with spinning sidebands (∗). Field is 9.4 T; MAS frequency, 4.2 kHz; repetition period, 20 s.

Table 1. Parameters of ^{17}O spectra of BaFBr:O (3%) and BaFCl:O (6%). Line position with reference to H_2O, MAS linewidth (FWHM), fractional intensity within centre band spectrum, spin/lattice relaxation time, upper bound to quadrupole coupling.

Host	$\delta' \times 10^6$	Width $\times 10^6$	Intensity (%)	T_1 (s)	$K_Q <$ (MHz)
BaFBr	634	5	4	8	1.5
	610	4	22	11	1.3
	597	4	5	3	1.2
	587	8	16	5	1.9
	198	25	52	1.8	3.3
BaFCl	181	12	27	2	2.2
	161	20	56	1.5	2.9
	8	73	17	1.0	5.5

respectively.

After the sample had aged at room temperature for a period of 530 days, the line at 181 ppm had decayed in intensity by about 40% while the line at 161 was unaffected.

3.4. ^1H NMR

The proton MAS spectra of BaFX:O are shown in figure 6. In each case there are a number of fairly narrow, overlapping lines with chemical shifts between 1 and 5 ppm. Results are given in table 2. The sideband patterns at several spin rates were compared with the static spectra (not shown) of BaFX:O and $BaX_2{:}2H_2O$. The strong sidebands of the main line in BaFCl:O (figure 6(*a*)) derive from a broad, symmetrical component, 54 kHz wide, in the static spectrum, which is similar to that of $BaCl_2.2H_2O$, 58 kHz wide. The sidebands in BaFBr:O are inconspicuous (figure 6(*b*)), and the static spectrum lacks the broad feature, about 67 kHz wide, that was found in $BaBr_2.2H_2O$.

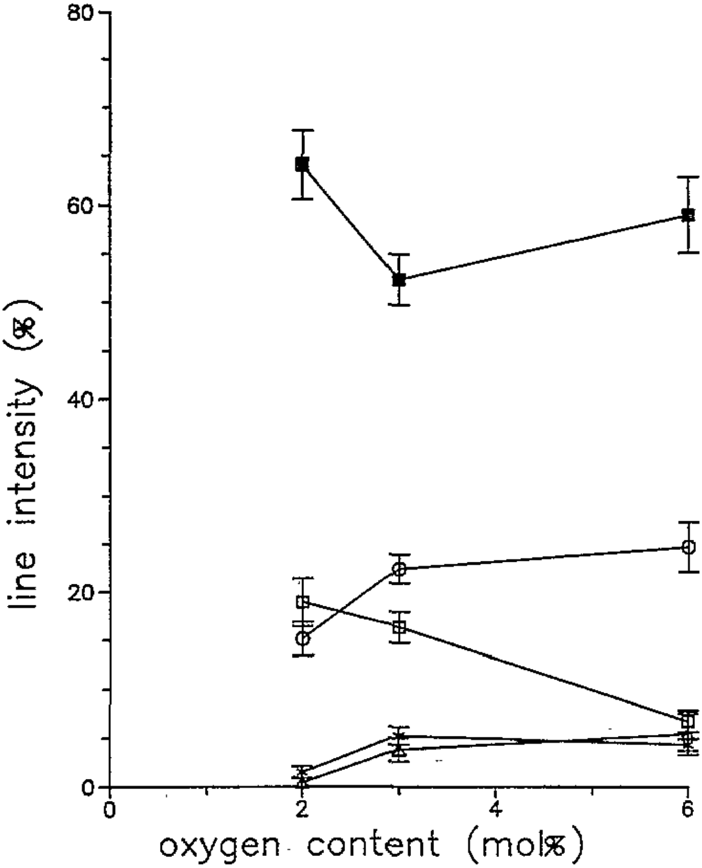

Figure 4. ^{17}O NMR absorption in BaFBr:O, relative line intensity as function of oxygen content. The line positions are approximately 630 (△), 610 (○), 597 (*), 587 (□), 197 (■) ppm.

4. Discussion

The halogen spectra show that the matrix into which the oxygen has been introduced remains fundamentally well ordered. The fluorine chemical shifts (section 3.1) are close to that in barium fluoride, which has also been reported as 215.5 (11) ppm (Burum *et al* 1978). Small amounts of BaF_2 or BaX_2 would not be detected.

The high resolution oxygen spectra reveal a number of well defined sites. In BaFBr:O there is one group of ^{17}O lines (figure 3) centred around 600 ppm, which is near the chemical shift of 629 ppm found in barium oxide, BaO (Turner *et al* 1985). The closest resemblance in BaFBr to the oxygen environment in BaO would be at the halide sites, although coordination by Ba is fivefold at Br, fourfold at F, rather than sixfold as in BaO. On general empirical grounds (Bastow and Stuart 1990), the chemical shift could be expected to increase as the coordination number is decreased from 6 to 4, as is observed in the case of La_2O_3. Presumably the observed shifts reflect the presence of second neighbours. It has been established by EPR in x-irradiated samples that the O^- radical occurs primarily at the fluoride site in BaFBr (Eachus *et al* 1991a, b). It is therefore reasonable to assign at least some of these NMR lines to O^{2-} on the F site (O_F^{2-}). The absence of Curie behaviour

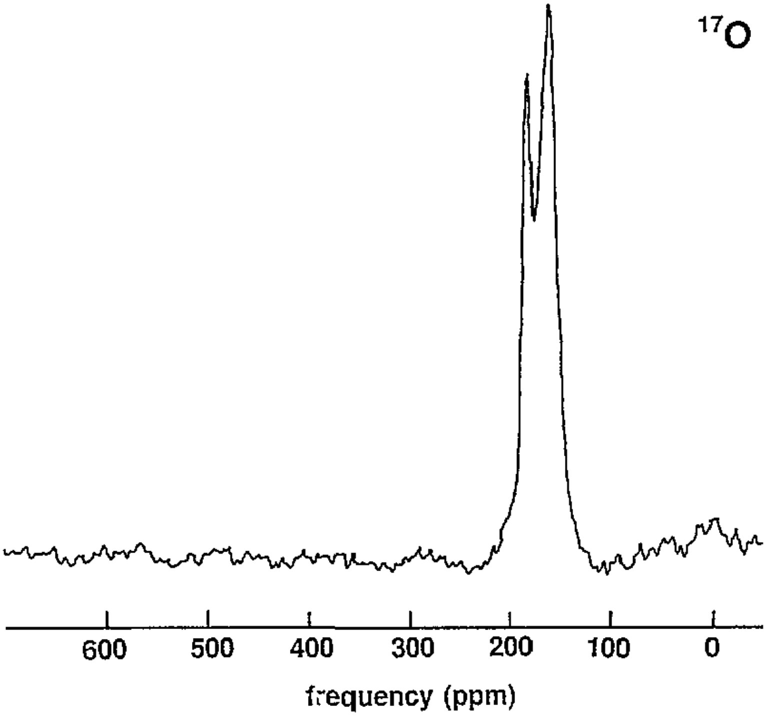

Figure 5. NMR spectrum of ^{17}O in BaFCl:O (6%) under magic-angle spinning (in silicon nitride spinner). Field is 9.4 T; MAS frequency, 4.7 kHz; repetition period, 10 s.

with temperature shows that the oxygen is not associated with any paramagnetic centre. The nutation behaviour shows that quadrupole interaction is present, although from the narrow linewidths it is rather small; indeed the F site has the highest symmetry ($\bar{4}m2$) in the perfect crystal. The assignment is also consistent with the crystallographic observation that oxygen occupies that position in bismuth oxyhalides, which share the matlockite structure (Sillén 1942). In addition there will be a charge-compensating vacancy at some halide site, which has been found to be a Br^- vacancy in close proximity to the O_F^{2-} (Koschnick *et al* 1991, 1992). The evidence came from the observation that, upon x-irradiation at temperatures below 120 K, $F(Br^-)$ centres were created which had their optical absorption band shifted to lower energy compared to the band from isolated F-centres. It could not be decided, however, whether the bromide vacancy was the nearest neighbour, the second-nearest neighbour or a combination of both configurations were present. Different positions of nearby vacancies would produce different chemical shifts at the oxygen. We tentatively assign the two strongest lines to O_F^{2-} associated with Br^- vacancies at the two nearest neighbour positions. One cannot be more specific without an elaborate chemical shift calculation.

O^{2-} has also been found on the Br site, during an EPR investigation (Eachus *et al* to be published) of x-irradiated, 'normally grown' BaFBr single crystals (Koschnick *et al* 1992). It was possible to remove the oxide by special treatment before crystal growth; when oxygen was reintroduced by BaO doping, however, only F-site oxide in the expected amount was found. It was speculated that the origin of the Br-site centre was an adventitious OH^- contamination, since the highest yield of O_{Br}^- could be achieved by irradiation with light at

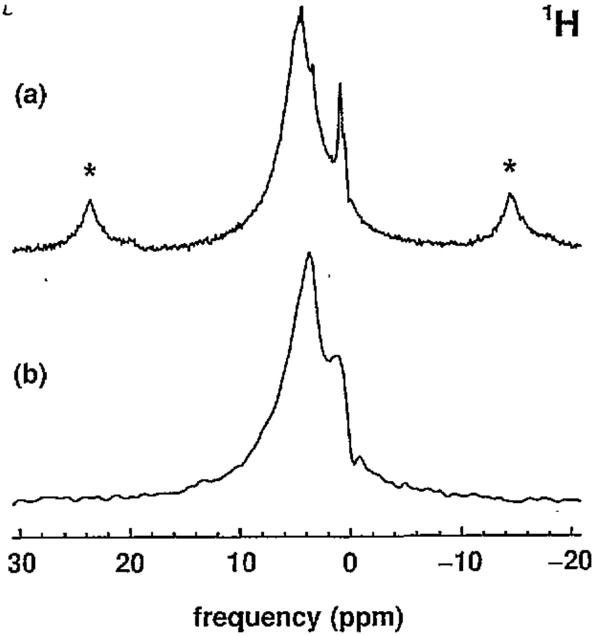

Figure 6. NMR spectra of ^1H in (*a*) BaFCl:O (6%), with MAS frequency 7.5 kHz; spinning sidebands (∗); (*b*) BaFBr:O (2%), with MAS frequency 10 kHz. Field is 9.4 T.

Table 2. Parameters of ^1H spectra of BaFBr:O (2%) and BaFCl:O (6%). Line position with reference to $Si(CH_3)_4$, MAS linewidth (FWHM), fractional intensity within centre band spectrum.

Host	$\delta' \times 10^6$	Width $\times 10^6$	Intensity (%)
BaFBr	3.9	4.1	92
	1.3	1.3	8
BaFCl	4.9	3.1	86
	3.6	0.6	3
	1.2	0.7	12

about 250 nm (Eachus *et al* to be published). Probably the present material has a similar contamination, which may account for the two weak NMR lines at 634 and 597 ppm as arising from O^{2-} on Br sites.

Most of the oxygen in BaFBr:O is found in the broader peak located considerably upfield at 198 ppm (figure 3). That is similar to the chemical shift of hydrogen peroxide, H_2O_2, which has been found in various states of dilution to be 174 (5) (Christ *et al* 1961), 179.5 (Bastow, unpublished data) and 187 (5) ppm (Figgis *et al* 1962). It may also be compared with barium peroxide, BaO_2, where the chemical shift of 334 ppm (Yang *et al* 1989) becomes $\delta' = 274$ ppm when the quadrupolar shift is added (Kundla *et al* 1981). The observed position is taken as evidence for the peroxide anion O_2^{2-}. Since the line does not narrow when the field is increased, as would have been expected from second-order quadrupole interaction, some distribution of sites is indicated. The linewidth sets an upper bound on the size of the quadrupole coupling (K_Q) of 3.3 MHz (table 1). Now that is much less than is found in solid hydrogen peroxide at 1.5 K, 17.55 (8) MHz (Lumpkin and

Dixon 1979), and in barium peroxide, 17.2 MHz (Yang *et al* 1989), where the molecule is fixed in position. Therefore we assign the line tentatively to interstitial O_2^{2-} ions that are able to reorient at room temperature, so reducing the average quadrupole coupling. It has been noted that after x-irradiation of BaFBr no superoxide radical O_2^- was detected by EPR, even at 4 K (in contrast to BaFCl, below). Either the charge state O_2^- is unstable in the interstitial position, or the molecule rotates too fast, or else it experiences a dynamic Jahn–Teller effect, so broadening the EPR line beyond recognition. We cannot exclude the possibility, however, of a substitutional O_2^{2-} which is similarly librating.

The null effect of x-irradiation may be due to the oxygen hole centres, which are known to be produced (Koschnick *et al* 1991), decaying in much less than 1 h at room temperature in these highly doped materials. The high O^{2-} concentration may facilitate the hole mobility through impurity-impurity interactions, shortening the life time of the paramagnetic O_F^- centres. Furthermore, the concentration of paramagnetic O^- centres produced by our x-irradiation (see section 2.1) is probably too low to be seen as a decrease of O^{2-} signals caused by O^{2-} impurities with a concentration of several mole percent.

The dramatic effect of annealing indicates that the oxide anions are less stable than the peroxide. The substitutional O^{2-} could relax to interstitial positions, where the electrostatic field gradient may be considerably increased. If the quadrupole coupling constant were greater than about 7 MHz, the spinning sidebands would overlap each other past recognition. It is also possible that under diffusion higher aggregates of oxygen are formed, which may elude detection.

The ^{17}O spectrum of BaFCl:O (figure 5) is strikingly different from that of BaFBr:O. No substitutional site around 600 ppm is detected, while around 170 ppm two presumably molecular lines appear instead of one. Observation of these resonances nutating at frequency $2.4\nu_1$ means that they are due to central transitions selectively excited. This puts a lower bound on the quadrupole frequencies (Cohen and Reif 1957), $|\nu_Q| \gtrsim 5\nu_1$, as deduced from figure 2 of Geurts *et al* (1985), and the coupling constants K_Q are therefore greater than about 1.9 MHz. Assuming the lines are separable, with no quadrupolar splitting, their linewidth allows us to calculate upper bounds to K_Q of 2.2 and 2.9 MHz (table 1), again much less than in the fixed peroxides. From the EPR of O_2^- there is evidence that the molecular anion is librating. EPR spectra of O_2^- could only be observed below 30 K, although the centres are stable at room temperature; this is a strong indication of motional effects above 30 K (Eachus *et al* 1993b). For instance, reorientation along the crystallographic axes a and b would average the electric field gradient (eq) at one of the nuclei of such a molecule to $-1/2$ times the static value. The postulated averaging of a static interaction implies a motional correlation time $\tau_c < T_2^* \simeq 0.4$ ms: while the measurement of a relaxation ratio $T_1/T_2 \simeq 10^2$ means that τ_c appreciably exceeds the nuclear Larmor time, $1/\omega_L = 2.9$ ps. When BaFCl was x-irradiated, in contrast to BaFBr, EPR detected the O_2^-, which on symmetry grounds was attributed to the chloride site, not to an interstitial (Eachus *et al* 1993b). We associate the narrower NMR line at 181 ppm with this substitutional molecular anion, and the broader line at 161 ppm with interstitial molecular anions, which are invisible in EPR, as for BaFBr:O, above (see table 1). We assume the differences are not due to associated vacancies. The shorter relaxation times of the broader line indicate a site of greater quadrupole interaction. The aging experience indicates that the interstitials are slightly more stable than the substitutional molecular anions. Thus NMR is able to detect impurity peroxide anions where they have escaped detection by EPR and optical spectroscopy. However, it must be noted, no electron paramagnetic resonance studies (EPR or ENDOR) have been carried out at such a high oxygen doping level. At the lower content of oxygen used in the EPR studies, 10 to 100 ppm, it was found after x-irradiation that the monatomic species O^- on the F site was much less prevalent than the molecular anions O_2^- on the Cl site, the concentration ratio being approximately 1:4 (Eachus *et al* to be published). At the present high content of oxygen, it seems that the molecular anion is even more favoured, and O_F^{2-} falls below the concentration limit of NMR detection, which is some orders of magnitude higher than it is with EPR.

The broadest ^{17}O line in BaFCl:O (figure 5) is the one about 0 ppm, which is characteristic of hydroxide groups (including water, the reference compound). It cannot be due to surface contamination, however, because the surface of the powder is not large enough. We assign this line to H_2O or OH^- which may be distributed in various sites within the crystal. The upper bound on the magnitude of the mean quadrupole coupling (table 1) is 5.5 MHz. That may be compared with β barium hydroxide at 77 K, 6.060 (5) and 6.568 (5) MHz, or barium hydroxide monohydrate at 77 K, 7.130 (8) and 6.691 (19) MHz (Poplett 1982a, b). That a similar line is not seen in BaFBr:O (figure 3) may be due to reduced signal strength.

The ^1H spectra (figure 6 and table 2) show at least two sites in BaFBr:O and BaFCl:O, one of which is common to both systems. The ^1H chemical shifts are all indicative of H_2O or OH^-. The line at 4.9 ppm in BaFCl:O is due to fixed water molecules, similar to those in $BaCl_2.2H_2O$ which are constrained by hydrogen bonds (Silvidi and McGrath 1960). We have observed that single crystals of both BaFBr and BaFCl show anisotropic voids which include the pure halides BaF_2, $BaCl_2$ or $BaBr_2$ while the surrounding material looks perfectly crystalline. The included $BaCl_2$ or $BaBr_2$ is hygroscopie—it swells on exposure to air, causing the crystals to fracture. The powders doped with high oxide levels would also have these inclusions. The ^1H evidence for water of crystallization in BaFCl is supported by the ^{17}O observation above. On the other hand, if water is the origin of the ^1H line at 3.9 ppm in BaFBr:O, it is not fixed in position but may be undergoing internal rotation. The smaller, sharper lines are probably due to OH^-. The presence of hydroxide species shows that the incorporation of oxygen into the crystal did not occur in a completely controlled manner. This helps to confirm an earlier suspicion (Eachus *et al* to be published) that the origin of O^- centres at Cl and Br sites is not O^{2-} under x-irradiation but OH^-, which is decomposed by light into O^- and H. The discovery of hydroxide may also explain our experience (unpublished) that those paramagnetic centres are not produced controllably by BaO doping.

5. Conclusion

We show the usefulness of NMR in detecting diamagnetic oxygen centres as impurities in inorganic solids. By using 40% isotopic enrichment of ^{17}O and magic-angle spinning to 5 kHz it is possible to detect an oxygen species if its concentration is more than 1000 ppm and if the quadrupole coupling constant is less than 7 MHz.

Previous EPR experience allows us to identify the probable species that appear in the ^{17}O NMR of BaFBr:O and BaFCl:O. In BaFBr:O the oxygen occurs as O^{2-} on both of the halide sites, though mainly the fluoride site, and also as O_2^{2-} possibly interstitially. In BaFCl:O at percent levels of doping, oxygen is found only in the molecular form, on the chloride site and interstitially. Interstitial O_2^{2-} has so far not been discussed as a possible participant in the radiographic process, although O_2^{2-} at the chloride site was already clearly evident from EPR (Eachus *et al* 1993b).

Despite great care having been taken in the preparation of our material, some hydroxide contamination apparently occurred. Such contamination may interfere with the functioning of x-ray storage phosphors based on BaFBr and BaFCl.

Acknowledgments

We are grateful to Dr D G Hay of CSIRO for the x-irradiation; to Dr M E Smith, University of Kent, for experimental advice, and to Dr S Steuernagel, Bruker Analytische Messtechnik, Rheinstetten, for the MSL 500 spectroscopy.

References

Amemiya G and Miyahara J 1988 *Nature* **336** 89

Bastow T J and Stuart S N 1990 *Chem. Phys.* **143** 459

Beck H P 1979 *Z. Anorg. (Allg.) Chem.* **451** 73

Burum D P, Elleman D D and Rhim W K 1978 *J. Chem. Phys.* **68** 1164

Christ H A, Diehl P, Schneider H R and Dahn H 1961 *Helv. Chim. Acta* **44** 865

Cohen M H and Reif F 1957 *Solid State Phys.* **5** 321

Eachus R S, Koschnick F K, Spaeth J-M, Nuttall R H D and McDugle W G 1993a *Proc. Int. Conf. on Defects in Insulating Materials (Nordkirchen, Germany)* ed O Kanert and J-M Spaeth (Singapore: World Scientific) p 267

Eachus R S, McDugle W G, Nuttall R H D, Olm M T, Koschnick F K, Hangleiter Th and Spaeth J-M 1991a *J. Phys.: Condens. Matter* **3** 9327; 1991b *J. Phys.: Condens. Matter* **3** 9339

Eachus R S, Nuttall R H D, McDugle W G, Koschnick F K and Spaeth J-M 1993b *Proc. Int. Conf. on Defects in Insulating Materials (Nordkirchen, Germany)* ed O Kanert and J-M Spaeth (Singapore: World Scientific) p 1172

Eachus R S, Nuttall R H D, McDugle W G, Koschnick F K and Spaeth J-M to be published

Figgis B N, Kidd R G and Nyholm R S 1962 *Proc. R. Soc.* A **269** 469

Geurts F M M, Kentgens A P M and Veeman W S 1985 *Chem. Phys. Lett.* **120** 206

Hangleiter Th, Koschnick F K, Spaeth J-M, Nuttall R H D and Eachus R S 1990 *J. Phys. C: Solid State Phys.* **2** 6837

Koschnick F K 1991 *Doctoral Thesis* University of Paderborn, Germany

Koschnick F K, Spaeth J-M and Eachus R S 1992 *J. Phys.: Condens. Matter* **4** 3015

Koschnick F K, Spaeth J-M, Eachus R S, McDugle W G and Nuttall R H D 1991 *Phys. Rev. Lett.* **67** 3571

Kotera N, Eguchi S, Miyahara J, Matsumoto S and Kato H 1980 *US Patent Specification* 4 239 968

Kundla E, Samoson A and Lippmaa E 1981 *Chem. Phys. Lett.* **83** 229

Liebich W B and Nicollin D 197 *Acta Crystallogr.* B **33** 2790

Luckey G W 1975 *US Patent Specification* 3 859 527; 1983 revised 31 847

Lumpkin O and Dixon W T 1979 *J. Chem. Phys.* **71** 3550

Poplett I J F 1982a *J. Magn. Reson.* **50** 382; 1982b *J. Magn. Reson.* **50** 397

Sauvage M 1974 *Acta Crystallogr.* B **30** 2786

Sillén L G 1942 *Naturwissenschaften* **30** 318

Silvidi A A and McGrath J W 1960 *J. Chem. Phys.* **32** 924

Sonoda M, Takano M, Miyahara J and Kato H 1983 *Radiology* **148** 835

Stevels A L N and Pingault F 1975 *Philips Res. Rep.* **30** 277

Takahashi K, Kohda K, Miyahara J, Kanemitsu Y, Amitani K and Shionoya S 1984 *J. Lumin.* **31, 32** 266

Takahashi K, Miyahara J and Shibahara Y 1985 *J. Electrochem. Soc.* **132** 1492

Turner G L, Chung S E and Oldfield E 1985 *J. Magn. Reson.* **64** 316

von Seggern H, Voigt T, Knüpfer W and Lange G 1988a *J. Appl. Phys.* **64** 1405

von Seggern H, Voigt T and Schwarzmichel K 1988b *Siemens Forsch.-und Entwickl.-Ber.* **17** 124

Yang S, Park K D and Oldfield E 1989 *J. Am. Chem. Soc.* **111** 7278